Title

Global and Regional Brain Non-Gaussian Diffusion Changes in Newly Diagnosed Patients with Obstructive Sleep Apnea

Journal

Sleep, 39(1)

ISSN

0161-8105

Authors

Tummala, Sudhakar
Palomares, Jose
Kang, Daniel W
et al.

Publication Date

2016

DOI

10.5665/sleep.5316

Peer reviewed

SLEEP DISORDERED BREATHING

Global and Regional Brain Non-Gaussian Diffusion Changes in Newly Diagnosed Patients with Obstructive Sleep Apnea

Sudhakar Tummala, PhD[1,*]; Jose Palomares, BS[1,*]; Daniel W. Kang, MD[2]; Bumhee Park, PhD[1]; Mary A. Woo, RN, PhD[3]; Ronald M. Harper, PhD[4,5]; Rajesh Kumar, PhD[1,5,6,7]

*[1]Department of Anesthesiology, [2]Department of Medicine, [3]UCLA School of Nursing, [4]Department of Neurobiology, [5]The Brain Research Institute, [6]Department of Radiological Sciences, and [7]Department of Bioengineering, University of California at Los Angeles. Los Angeles, CA; *co-first authors*

Study Objectives: Obstructive sleep apnea (OSA) patients show brain structural injury and functional deficits in autonomic, affective, and cognitive regulatory sites, as revealed by mean diffusivity (MD) and other imaging procedures. The time course and nature of gray and white matter injury can be revealed in more detail with mean kurtosis (MK) procedures, which can differentiate acute from chronic injury, and better show extent of damage over MD procedures. Our objective was to examine global and regional MK changes in newly diagnosed OSA, relative to control subjects.

Methods: Two diffusion kurtosis image series were collected from 22 recently-diagnosed, treatment-naïve OSA and 26 control subjects using a 3.0-Tesla MRI scanner. MK maps were generated, normalized to a common space, smoothed, and compared voxel-by-voxel between groups using analysis of covariance (covariates; age, sex).

Results: No age or sex differences appeared, but body mass index, sleep, neuropsychologic, and cognitive scores significantly differed between groups. MK values were significantly increased globally in OSA over controls, and in multiple localized sites, including the basal forebrain, extending to the hypothalamus, hippocampus, thalamus, insular cortices, basal ganglia, limbic regions, cerebellar areas, parietal cortices, ventral temporal lobe, ventrolateral medulla, and midline pons. Multiple sites, including the insular cortices, ventrolateral medulla, and midline pons showed more injury over previously identified damage with MD procedures, with damage often lateralized.

Conclusions: Global mean kurtosis values are significantly increased in obstructive sleep apnea (OSA), suggesting acute tissue injury, and these changes are principally localized in critical sites mediating deficient functions in the condition. The mechanisms for injury likely include altered perfusion and hypoxemia-induced processes, leading to acute tissue changes in recently diagnosed OSA.

Keywords: acute injury, diffusion kurtosis imaging, hypoxia, obstructive sleep apnea

Citation: Tummala S, Palomares J, Kang DW, Park B, Woo MA, Harper RM, Kumar R. Global and regional brain non-gaussian diffusion changes in newly diagnosed patients with obstructive sleep apnea. *SLEEP* 2016;39(1):51–57.

Significance

Diffusion kurtosis imaging-based non-Gaussian mean kurtosis procedures are more sensitive to tissue injury than the more-commonly used diffusion tensor imaging-based Gaussian mean diffusivity measures in obstructive sleep apnea (OSA). That sensitivity allows better, and earlier detection of damage in the condition. Moreover, the procedures better differentiate acute from chronic stages of pathology, an aspect essential to determine the processes of injury in OSA, and to determine the effectiveness of ventilatory support or other interventions on brain tissue changes.

INTRODUCTION

Obstructive sleep apnea (OSA) is characterized by partial or complete obstruction of the upper airway, with continued diaphragmatic effort during sleep.[1] Brain structural changes and altered functional magnetic resonance imaging (MRI) signals to autonomic and ventilatory challenges appear in OSA subjects in cognitive, mood, and autonomic control areas, limbic regions, and likely contribute to the enhanced sympathetic tone, hypertension, and cardiac arrhythmias in the syndrome.[2,3] Abnormal autonomic, cognitive, and mood deficits are also common in OSA subjects, and presumably result from injury in those regulatory structures.[2,4] The structural injuries were initially identified with multiple MRI procedures, including diffusion tensor imaging (DTI)-based techniques in OSA subjects with long-standing impaired breathing,[5] but overall extent and nature of pathological damage in newly diagnosed, treatment-naive patients with OSA remains unclear.

DTI, based on Gaussian diffusion phenomena, is a technique for characterization of microstructural tissue changes, and has been valuable for elucidating the location and extent of injury in OSA, especially to fibers damaged in the condition.[6] DTI procedures characterize white matter using local estimates of fiber orientations. However, water diffusion in brain tissue is non-Gaussian in nature, due to the presence of cellular microstructures, myelinated axons, and minimal spacing between fibers that cross in many brain areas, leading the DTI procedures to inadequately assess complete diffusion properties of those sites.[7] A recently developed technique, diffusion kurtosis imaging (DKI), previously unused in OSA studies, is a significant improvement over the DTI model to assess non-Gaussian diffusion properties. The DKI metrics quantify the degree of non-Gaussian diffusion, provide a second-order approximation of water diffusion in both gray and white matter tissue,[8] and are closely related to tissue microstructure. Several DKI metrics, including mean kurtosis (MK), which indicates the average amount by which the diffusion displacement probability distribution deviates from Gaussian diffusion within tissue, can be calculated, and used to examine non-Gaussian tissue properties.

A principal advantage of MK measures, in addition to better assessment of extent of injury, is that they assist differentiation of acute from chronic injury.[9] Such differentiation is a critical aspect for studies of neural injury in OSA, since a major concern is whether the neural damage results from recent exposure to hypoxia and other physiological consequences accompanying apnea, or develops from long-standing breathing disturbances. MK measures have shown promising insights into the

developmental time course and extent of injury in other brain diseases, including stroke,[10] staging of glioblastomas,[11] and attention-deficit hyperactivity disorder,[12] and normal aging.[13] Thus, the advantages that the MK procedure have brought to those other pathologies may be equally useful for OSA studies.

Our aim was to examine global and regional MK values in recently diagnosed, without-treatment OSA, compared to control subjects. We hypothesized that global MK values will be increased in OSA, since we expect acute tissue injury in early stages of the syndrome, and that localized increases will appear in multiple brain regions that control deficient functions in the condition.

METHODS

Participants

We studied 22 OSA (age, 49.2 ± 8.4 y; body mass index [BMI], 32.9 ± 7.9 kg/m^2; 16 male; apnea-hypopnea index [AHI], 43.1 ± 28.3 events/h) and 26 healthy control subjects (age, 45.6 ± 9.3 y; BMI, 25.4 ± 3.6 kg/m^2; 15 male). OSA subjects were recently diagnosed through overnight polysomnography (PSG) with at least mild severity (AHI ≥ 5), were treatment-naive, and recruited from the Sleep Disorders Laboratory at the University of California Los Angeles (UCLA) Medical Center. All OSA subjects were not on any cardiovascular-altering medications, such as β-blockers, α-agonists, angiotensin-converting enzyme inhibitors, and vasodilators, or mood altering drugs, e.g., serotonin reuptake inhibitors. OSA subjects with a history of stroke, with a diagnosis of any brain conditions, heart failure, metallic implants, or any contraindication on brain imaging were excluded from the study. Control subjects were in good health, without any history of neurological or other brain disorders or any medications that might alter brain tissue, had no evidence of sleep disorders (normal scores on the Epworth Sleepiness Scale [ESS]), and were recruited through advertisements at the UCLA campus and neighboring community. All study procedures were approved by the Institutional Review Board of the UCLA, and each subject provided written informed consent prior to participate in the study.

Overnight PSG

All OSA subjects underwent overnight sleep studies at the UCLA Sleep Disorders Laboratory with standard procedures, consisting of a 7- to 10-h monitoring period of electroencephalogram (central and occipital), digastric electromyogram, electrocardiogram (lead II), right and left extraocular eye movement, thoracic and abdominal wall movement, air flow, O_2 saturation, end-tidal CO_2 levels, snore volume, bilateral leg movement, and sleep position. All acquired PSG data were digitized and stored on a computer for further sleep evaluation.

Assessment of Sleep Quality and Daytime Sleepiness

All OSA and control subjects were evaluated for sleep quality with the Pittsburgh Sleep Quality Index (PSQI), and daytime sleepiness with the ESS. Both questionnaires are self-administered tests, and are commonly used tools to examine sleep quality and daytime sleepiness.[14]

Evaluation of Depression and Anxiety Symptoms

We used the Beck Anxiety Inventory (BAI) and Beck Depression Inventory II (BDI-II) questionnaires for assessment of anxiety[15] and depressive[16] symptoms, respectively, in OSA and control subjects. Both tools are self-administered questionnaires (21 questions; each score ranged from 0–3), with total scores ranging from 0–63 based on symptom severity.

Cognition Assessment

We used the Montreal Cognitive Assessment (MoCA) test for cognitive assessment. The MoCA test is designed for fast screening of various cognitive domains, including attention and concentration, executive functions, memory, language, visuoconstructional skills, conceptual thinking, calculations, and orientation.[17]

Magnetic Resonance Imaging

Brain structural imaging studies were performed using a 3.0-Tesla MRI scanner (Siemens; Magnetom Tim-Trio, Erlangen, Germany). High-resolution T1-weighted images were acquired using a magnetization-prepared rapid acquisition gradient echo pulse sequence in the sagittal plane [repetition time (TR) = 2200 msec; echo time (TE) = 2.34 msec; inversion time = 900 msec; flip angle (FA) = 9°; matrix size = 320 × 320; field of view (FOV) = 230 × 230 mm; slice thickness = 0.9 mm; slices = 192]. Proton-density and T2-weighted images were collected using a dual-echo turbo spin-echo pulse sequence in the axial plane (TR = 10,000 msec; TE1, 2 = 17, 134 ms; FA = 130°; matrix-size = 256 × 256; FOV = 230 × 230 mm; slice thickness = 3.5 mm). Diffusion kurtosis imaging data were acquired using an echo planar imaging with twice-refocused spin echo pulse sequence in the axial plane (TR = 7000 msec; TE = 90 msec; FA = 90°; bandwidth = 2439 Hz/pixel; matrix-size = 82 × 82; FOV = 230 × 230 mm; slice thickness = 2.8 mm; 60 slices; no interslice-gap; duration of diffusion gradient = ~35 msec; temporal spacing between two diffusion gradients = ~7.5 msec; diffusion directions = 30; b values = 0, 1000, and 2000 s/mm^2), and two separate series were collected for subsequent averaging.

Data Processing and Analyses

Overnight PSG Data

Sleep data were scored by an expert PSG technician, and each PSG was reviewed by a sleep physician. Sleep states, sleep disordered breathing, and physiology were assessed first, for total sleep time, number, and type (central, obstructive, or mixed--based on airflow and thoracic and abdominal strain gauges) of apneic episodes. Scoring was based on recently revised scoring criteria.[18] The AHI is a severity index of sleep disordered breathing, combining both apneas and hypopneas, and is calculated by dividing the number of apnea and hypopnea by the total sleep time. Subjects were categorized as having OSA based on an AHI ≥ 5 events/h.[19] An OSA subject was categorized as "mild" OSA, if AHI was ≥ 5 events/h, but < 15 events/h, categorized as "moderate," if AHI ≥ 15 events/h, but < 30 events/h, and "severe" if AHI ≥ 30 events/h.[19] The total number and duration of apnea, AHI, number of arousals, O_2 saturation variables, total sleep time, time in each state, and sleep efficiency variables were calculated.

MRI Data

The statistical parametric mapping package SPM8 (http://www.fil.ion.ucl.ac.uk/spm/), Diffusional Kurtosis Estimator (DKE) software (Neuroimaging Informatics Tools and Resources, Clearinghouse, v 2.5.1),[20] MRIcroN,[21] and MATLAB-based (http://www.mathworks.com/) custom-written software were used for data processing and analyses. We used high-resolution T1-, PD-, and T2-weighted images of OSA and control subjects to examine for any visible brain tissue pathology, such as tumors, cysts, or any other major mass lesion. Diffusion- and nondiffusion-weighted images of all subjects were also assessed for any head–motion-related or other imaging artifacts before MK calculation. No subjects (OSA or controls) included in this study showed any major visible brain pathology, head motion, or other imaging artifacts.

Calculation of MK Maps

MK maps were derived from diffusion (b = 1000 and 2000 sec/mm^2) and nondiffusion (b = 0 sec/mm^2) data using the DKE software.[20] We performed motion correction using rigid-body transformation with six parameters to spatially align all diffusion-weighted images, and the diffusional kurtosis tensors were mutually fitted to the diffusion-weighted images (b = 0, 1000 and 2000 sec/mm^2) for each voxel. MK maps were calculated from the diffusion kurtosis tensor of each DKI series from individual subjects.[20]

Realignment, Averaging, Normalization, and Smoothing

We realigned both MK maps, computed from each DKI series, to remove any differences in alignment, resulting from potential head motion. Both realigned MK maps were averaged to create one MK map per subject. Similarly, nondiffusion-weighted images (b0 images) were also realigned and averaged. The averaged MK maps were normalized to Montreal Neurological Institute (MNI) space using normalization information derived from b0 images. The averaged b0 images were partitioned into gray matter, white matter, and cerebrospinal fluid (CSF) tissue types, based on a *priori* defined distributions of tissue types,[22] and the resulting normalization parameters were applied to corresponding MK maps, b0 images, and gray, white, and CSF tissue probability maps. The normalized MK maps were smoothed with an isotropic Gaussian filter (10-mm kernel). We also normalized higher resolution T1-weighted image of a control subject to create a whole-brain mean background image for structural identification.

Global Brain Mask

The normalized white matter probability maps from OSA and control subjects were averaged, and similarly, the normalized gray matter probability maps from all subjects were averaged. The averaged gray and white matter probability maps were thresholded (white matter probability > 0.3, gray matter probability > 0.3), and combined to create a global brain mask.

Global Brain MK Calculation

We masked nonbrain regions (CSF and other nonbrain areas) from the normalized MK maps of all individuals using a global brain mask. The masked MK maps were used to calculate mean global brain MK values from OSA and control subjects using MATLAB-based custom-written software.

Statistical Analysis

Data analyses were performed using the International Business Machines statistical package for the social sciences software (IBM SPSS, Armonk, New York, v22). Demographic, biophysical, sleep variables, neuropsychologic, and cognitive scores were compared between groups using independent samples *t*-tests and Chi-square tests. Global brain MK values were compared between groups using analysis of covariance (ANCOVA), with age and sex included as covariates. A value of $P < 0.05$ was chosen to establish statistical significance.

The normalized and smoothed MK maps were compared voxel-by-voxel between OSA and control groups using ANCOVA (covariates, age and sex; SPM8, uncorrected threshold, $P < 0.005$). We did not apply a cluster level threshold; however, we did not report any brain sites with fewer than five clusters. Brain sites with significant differences between OSA and control groups were overlaid onto whole-brain background images for structural identification.

RESULTS

Demographic, Biophysical, and Physiological Data

Demographic, biophysical, and physiological data are summarized in Table 1. No significant differences in age ($P = 0.16$), sex ($P = 0.28$), education ($P = 0.97$), heart rate ($P = 0.35$), and diastolic blood pressure ($P = 0.06$) were present between groups. However, body mass indices ($P < 0.001$) and systolic blood pressure values ($P = 0.008$) were significantly higher in OSA subjects.

Sleep, Overnight PSG, Affective, and Cognitive Variables

Sleep, overnight PSG, affective, and cognitive variables of OSA and control subjects are summarized in Table 1. ESS and PSQI scores were significantly higher in OSA, compared to control subjects (ESS, $P < 0.001$; PSQI, $P < 0.001$). BDI-II scores were significantly higher in OSA over control subjects ($P = 0.046$); however, BAI scores did not differ significantly ($P = 0.079$). Global MoCA scores did not significantly differ between groups ($P = 0.053$), but significant differences emerged in the visuospatial domain scores between OSA and control subjects ($P = 0.009$).

Global MK Changes

The global brain average MK value in control subjects was 0.856 ± 0.027, and in OSA subjects was 0.875 ± 0.034. The global brain MK values were significantly increased in OSA over control subjects ($P = 0.03$).

Regional Brain MK Changes

Multiple brain areas in OSA showed increased MK values, compared to control subjects (Figures 1 and 2). No brain sites showed decreased MK values in OSA over control subjects. Brain regions that showed increased MK values in OSA subjects included the bilateral hippocampus and amygdala (Figures 1, a and b), bilateral cerebellar vermis (Figure 1, c),

Table 1—Demographic, biophysical, sleep, and mean global mean kurtosis of obstructive sleep apnea and control subjects.

Variable Type	Variables	OSA	Controls	P
Demographic	Age (y)	49.2 ± 8.4 (n = 22)	45.6 ± 9.3 (n = 26)	0.159
	Sex (male: female)	16:6 (n = 22)	15:11 (n = 26)	0.278
	Education	16 ± 1.87 (n = 19)	18.28 ± 3.7 (n = 25)	0.971
Biophysical	BMI (kg/m^2)	32.9 ± 7.9 (n = 22)	25.4 ± 3.6 (n = 26)	< 0.001
Physiological	Hear rate (beats/min)	78.6 ± 12.2 (n = 19)	74.7 ± 14.5 (n = 24)	0.352
	Systolic BP (mmHg)	128.7 ± 15.0 (n = 19)	115.5 ± 15.8 (n = 24)	0.008
	Diastolic BP (mmHg)	79.9 ± 9.7 (n = 19)	73.7 ± 11.4 (n = 24)	0.065
Sleep	PSQI	7.8 ± 3.9 (n = 22)	3.6 ± 3.0 (n = 26)	< 0.001
	ESS	7.8 ± 3.9 (n = 22)	3.9 ± 3.0 (n = 26)	< 0.001
Affective	BDI-II	5.1 ± 4.6 (n = 22)	2.7 ± 3.4 (n = 26)	0.046
	BAI	4.5 ± 4.5 (n = 22)	2.5 ± 3.3 (n = 26)	0.079
Cognitive	Global MoCA scores	25.6 ± 4.5 (n = 19)	27.8 ± 2.2 (n = 24)	0.053
	MoCA: Visuospatial	3.7 ± 1.3 (n = 19)	4.6 ± 0.6 (n = 24)	0.009
	MoCA: Naming	2.9 ± 0.3 (n = 19)	2.8 ± 0.5 (n = 24)	0.634
	MoCA: Attention	5.3 ± 1.3 (n = 19)	5.7 ± 0.6 (n = 24)	0.234
	MoCA: Language	2.4 ± 0.8 (n = 19)	2.6 ± 0.8 (n = 24)	0.514
	MoCA: Abstraction	1.8 ± 0.4 (n = 19)	2.0 ± 0.0 (n = 24)	0.083
	MoCA: Delayed recall	3.6 ± 1.5 (n = 19)	4.2 ± 1.0 (n = 24)	0.161
	MoCA: Orientation	5.9 ± 0.3 (n = 19)	6.0 ± 0.2 (n = 24)	0.428
Overnight PSG data	AHI (events/h)	43.1 ± 28.3 (n = 22)	_	_
	Baseline SaO_2 (%)	94.9 ± 1.9 (n = 21)	_	_
	SaO_2 nadir (%)	76.8 ± 8.7 (n = 21)	_	_
	SaO_2 nadir change (%)	18.2 ± 8.1 (n = 21)	_	_
	Arousal index	36.7 ± 24.7 (n = 19)	_	_
	Sleep efficiency index	79.8 ± 14.5 (n = 20)	_	_
Global MK values	Global mean kurtosis	0.875 ± 0.034 (n = 22)	0.856 ± 0.027 (n = 26)	0.031

AHI, apnea-hypopnea index; BAI, Beck Anxiety inventory; BDI-II, Beck Depression Inventory II; BMI, body mass index; BP, blood pressure; ESS, Epworth Sleepiness Scale; MoCA, Montreal Cognitive Assessment; OSA, obstructive sleep apnea; PSG, polysomnography; PSQI, Pittsburgh Sleep Quality Index; SaO_2, oxygen saturation; SD, standard deviation.

right middle cerebellar peduncle (Figure 1, d), basal forebrain (Figure 1, n), left cerebellar cortex (Figure 1, m), right ventrolateral medulla (Figure 1, h), bilateral temporal lobes (Figure 1, g and p), midline pons (Figures 1, i, l, and f), left mid temporal lobe (Figure 1, j), right posterior parietal lobe (Figure 1, k), and right occipital cortex (Figure 1, q). Other areas with increased MK values appeared in the anterior, mid, and posterior insular cortices (Figure 2, a), left anterior internal capsule (Figure 2, c), bilateral parietal cortices (Figure 2, b, d, and f), right external capsule and putamen (Figure 2, a), bilateral prefrontal cortices (Figure 2, e and i), right medial parietal cortex (Figure 2, h), and right motor cortex (Figure 2, g).

DISCUSSION

Overview

Newly diagnosed, treatment-naive OSA subjects showed significantly different sleep, neuropsychologic, and cognitive values compared to controls. Based on voxel-based analyses, OSA subjects showed significantly increased global MK values, and these changes were localized in various brain areas critical for autonomic, cognitive, motor, and respiratory control functions, including the basal forebrain, hippocampus, amygdala, insular cortices, basal ganglia, limbic regions, cerebellar areas, parietal cortices, temporal lobe, ventrolateral medulla, and midline pontine sites, suggesting acute tissue changes in those regions. The pathological mechanisms contributing to tissue damage may stem from a range of hypoxic, hypercapnic, or perfusion changes accompanying apnea.

OSA and Brain Tissue Injury

OSA subjects show brain abnormalities and metabolic deficits in multiple areas, based on both conventional and advanced MRI and spectroscopy procedures. Gray matter tissue loss or injury appears in the anterior and posterior cingulate and insular cortices, mammillary bodies, hippocampus, bilateral caudate, putamen, and thalamus, cerebellar cortex and deep nuclei, and frontal, parietal, and temporal regions; metabolic

deficits appear in several sites.[2,5,23,24] Fiber injury emerges in the corpus callosum, cingulum bundle, fornix, internal capsule, cerebellum and peduncles, and corticospinal tract, and frontal white matter regions show compromised brain metabolites.[5] The initial evaluation of types of tissue damage included examination by mean diffusivity (MD) procedures; we now add MK assessment, which provides insights into the time course of injury and a more precise evaluation of damage in localized areas.

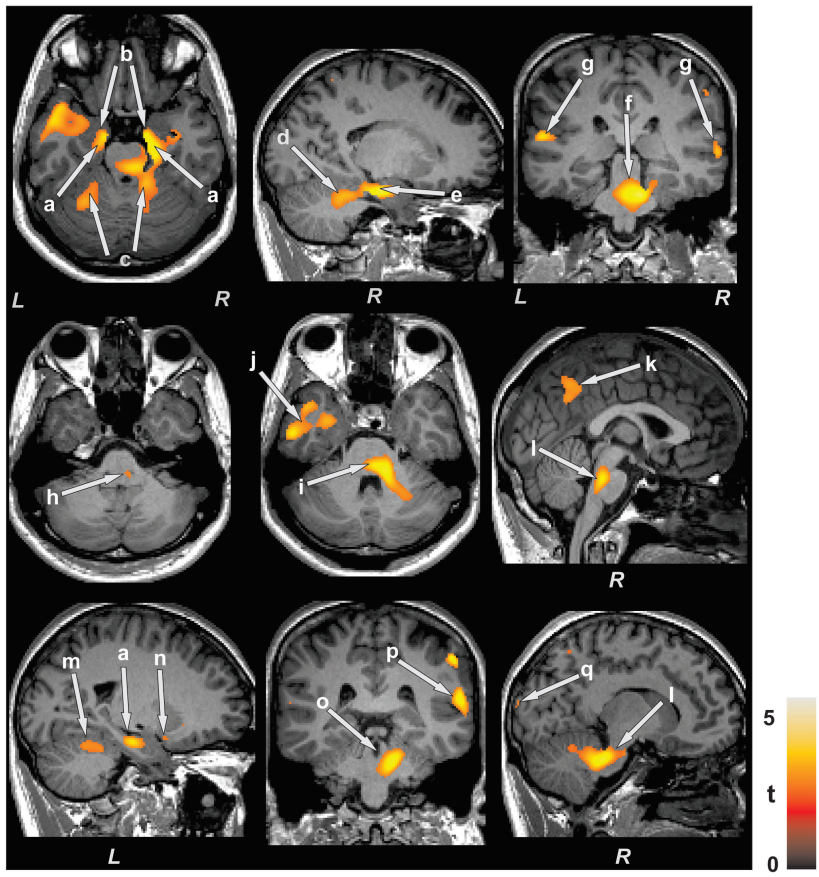

Figure 1—Brain regions with increased regional mean kurtosis values in obstructive sleep apnea compared to control subjects. These sites included the bilateral hippocampus and amygdala (a, b), bilateral cerebellar vermis (c), right middle cerebellar peduncle (d), basal-forebrain (n), left cerebellar cortex (m), right ventrolateral medulla (h), bilateral temporal lobes (g, p), midline pons (f, i, l), left mid temporal lobe (j), right posterior parietal lobe (k), and right occipital cortex (q).

Increased MK and Nature of Brain Damage

Multiple brain areas in OSA showed increased regional MK values, a biomarker of tissue heterogeneity, compared to control subjects. Ischemic lesions, resulting from stroke in both gray and white matter, showed higher MK values in acute conditions (12 h to 5 d), compared to normal tissue. Such an increase in MK values is suggested to emerge from a higher complexity/heterogeneity of water diffusion caused by focal enlargement of axons and dendrites, resulting from an osmotic imbalance due to energy failure from an ischemic condition. These morphologic axonal and cellular changes resulting from an osmotic imbalance lead to axonal and cellular swelling, and may be responsible for regional increases in MK values. Other human studies in cerebral infraction[10] and animal studies in traumatic brain injury showed increased MK values of neuronal tissue in subacute stages, and findings with increased MK values are interpreted as an association with higher reactive astrogliosis.[25,26] In this study, increased global and regional MK values likely result from neural tissue volume fraction changes (cytotoxic edema and axonal and neuronal swelling), causing impaired cell membrane permeability and energy pump failure, secondary to ischemic/hypoxia, suggesting acute tissue damage in these newly diagnosed OSA subjects.

Previous studies showed brain changes with only obesity and hypertension conditions.[27–30] The OSA subjects included here showed enhanced BMI and blood pressure variables over controls. We did not partition for such contributions in our analyses, and some of the findings may derive from the increased BMI and blood pressure.

MD Versus MK and Tissue Damage

Earlier studies showed reduced MD values in recently diagnosed, treatment-naive OSA subjects, implying acute tissue pathology at an early stage of the disease. In this study, we observed significantly increased MK values in multiple brain areas, which also suggest the presence of acute tissue injury. However, various brain areas, including the insular cortices, basal forebrain, ventrolateral medulla, and midline pons, showed more widespread damage compared to previously identified MD changes. MK measures tissue in a non-Gaussian fashion, and is influenced by the cellular microenvironment, myelin and neuronal integrity, and other tissue heterogeneity. Multiple studies with hypoxia/ischemia-induced injury in acute stages showed increased MK values.[31,32] However, examination of both MD and MK values in acute and sub-acute stages indicated that MD values at the acute stage were significantly reduced, and MK values were significantly increased, while in the subacute stage, MD values returned to normal, although MK values remained higher, suggesting the presence of a pathological condition, and a more sensitive attribute of MK over MD for detection of pathology. MK is a more accurate measure for detection of intracellular tortuosity and viscosity changes, subsequent to breakdown of cytoskeleton structures and axonal and cellular swelling. Different biological processes are attributable to hypoxia/ischemia-induced gray and white matter changes,[33] and various studies show the appearance of ischemic abnormalities on MK, but not on MD measures. In this study, the insular cortices and basal forebrain, ventrolateral medulla, and midline pons showed more lateralized MK

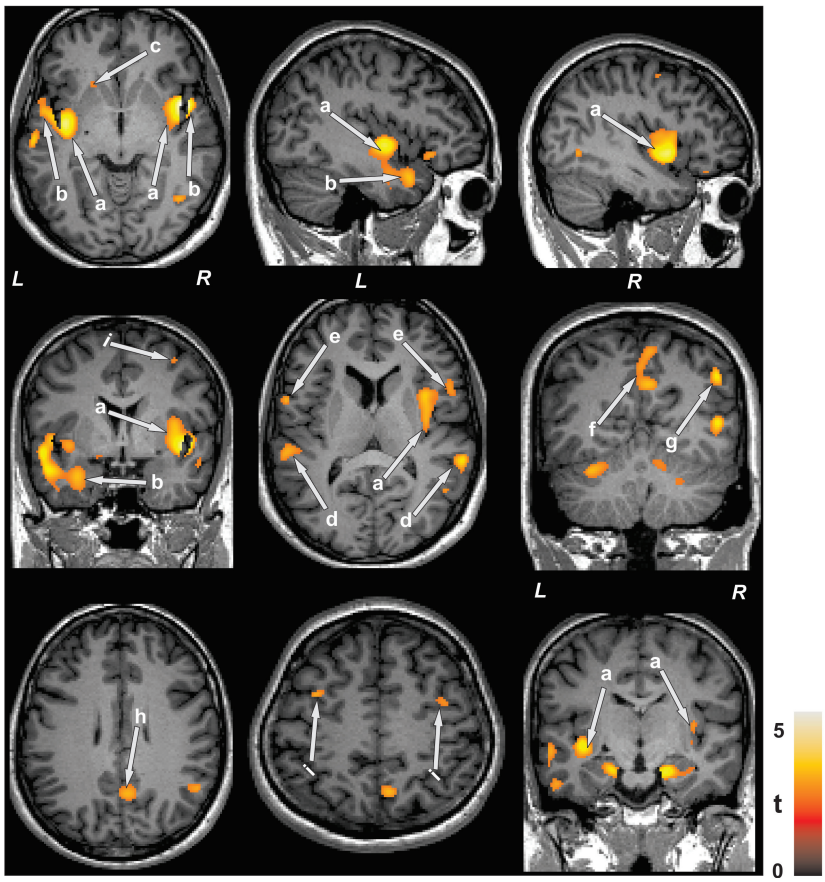

Figure 2—Brain areas with increased regional mean kurtosis values in obstructive sleep apnea over control subjects. Sites included the left, mid, posterior, and right anterior, mid, and posterior insular cortices (a), left anterior internal capsule (c), bilateral parietal cortices (b, d, f), right external capsule and putamen (a), bilateral prefrontal cortices (e, i), right medial parietal cortex (h), and right motor cortex (g).

changes, compared to previously detected MD changes, indicating more severe damage in these autonomic and respiratory regulatory sites.

Brain Injury in Autonomic, Respiratory, and Neuropsychologic Regulatory Sites

This study shows significantly increased MK values in specific brain sites responsible for regulation of autonomic, respiratory, and neuropsychologic functions. The basal forebrain, ventrolateral medulla, and midline pons, sites essential for blood pressure, chemosensation, respiratory regulation, and integration of baroreceptor and chemoreceptor afferents, showed widespread damage. Previous studies also observed abnormalities in these sites, but were based on measures that followed a Gaussian distribution, and showed less injury. The bilateral insular cortices, areas that influence both sympathetic and parasympathetic outflow, showed extensive injury, compared to previously identified damage, indicating the potential for severe autonomic distortions. Additionally, the basal forebrain, ventrolateral medulla, and midline pons, sites that control breathing and autonomic functions, also showed more widespread damage. A range of previously described injury in other brain sites also showed injury with MK measures, confirming damage in those regions.

Lateralization of Injury and Functional Consequences

Tissue injury was lateralized in several sites, including the right insular cortices, left hippocampus, and right ventrolateral medulla; lateralization of many brain functions is a well-known phenomenon in humans. The right insular cortex plays a significant role in regulating sympathetic nervous system output and modulating the baroreflex, an especially important concern in sleep disordered breathing, whereas the left insular cortex principally mediates parasympathetic nervous system activity, which decreases heart rate and blood pressure.[34] The greater injury found in the right insula may contribute to enhanced sympathetic discharge, enhancing the potential for cardiac dysrhythmia and altering brain perfusion in OSA. The left hippocampus is an integral component of the medial frontal cortex-hippocampal network for blood pressure control,[35] and the right ventrolateral medulla is the principal final output path before the sympathetic intermediolateral column of the spinal cord. The consequences of such lateralization of damage raise the possibility of asymmetric sympathetic outflow, and thus, a higher risk for cardiac arrhythmia in addition to hypertension. The loss of restraining influences normally mediated by a now-damaged right insular cortex on hypothalamic sympathetic regulation will alter release of multiple hormones, including glycogon and cortisol, both significantly disturbed in OSA. Both the extent of injury in these autonomic areas, as well as lateralization must be considered for consequences to pathophysiology.

CONCLUSIONS

Global brain MK values are significantly increased in newly diagnosed, treatment-naive OSA over control subjects, suggesting that the tissue changes are largely in the acute stage of injury. Regional MK changes, reflected as higher MK values in OSA, are localized in the basal forebrain, basal ganglia, limbic, and cerebellar sites, regions that are critical for autonomic, cognitive, motor, and respiratory control. Many brain areas, including the insular cortices, basal forebrain, ventrolateral medulla, and midline pons, emerged with more wide-spread injury over previously shown MD abnormalities, suggesting more severe damage in autonomic and respiratory regulatory regions. The lateralization of injury raises the potential for significant consequences to autonomic, and especially sympathetic outflow, with risks for cardiac arrhythmia, hypertension, and hormone release. The pathological mechanisms

contributing to tissue injury likely include hypoxic, hypercarbic, and perfusion processes leading to acute tissue changes.

REFERENCES

1. Strollo PJ, Jr., Rogers RM. Obstructive sleep apnea. N Engl J Med 1996;334:99–104.
2. Macey PM, Kumar R, Woo MA, Valladares EM, Yan-Go FL, Harper RM. Brain structural changes in obstructive sleep apnea. Sleep 2008;31:967–77.
3. Henderson LA, Woo MA, Macey PM, et al. Neural responses during Valsalva maneuvers in obstructive sleep apnea syndrome. J Appl Physiol 2003;94:1063–74.
4. Kumar R, Macey PM, Cross RL, Woo MA, Yan-Go FL, Harper RM. Neural alterations associated with anxiety symptoms in obstructive sleep apnea syndrome. Depress Anxiety 2009;26:480–91.
5. Kumar R, Chavez AS, Macey PM, Woo MA, Yan-Go FL, Harper RM. Altered global and regional brain mean diffusivity in patients with obstructive sleep apnea. J Neurosci Res 2012;90:2043–52.
6. Alexander AL, Lee JE, Lazar M, Field AS. Diffusion tensor imaging of the brain. Neurotherapeutics 2007;4:316–29.
7. Lu H, Jensen JH, Ramani A, Helpern JA. Three-dimensional characterization of non-gaussian water diffusion in humans using diffusion kurtosis imaging. NMR Biomed 2006;19:236–47.
8. Jensen JH, Helpern JA, Ramani A, Lu H, Kaczynski K. Diffusional kurtosis imaging: the quantification of non-gaussian water diffusion by means of magnetic resonance imaging. Magn Reson Med 2005;53:1432–40.
9. Hui ES, Fieremans E, Jensen JH, et al. Stroke assessment with diffusional kurtosis imaging. Stroke 2012;43:2968–73.
10. Jensen JH, Falangola MF, Hu C, et al. Preliminary observations of increased diffusional kurtosis in human brain following recent cerebral infarction. NMR Biomed 2011;24:452–7.
11. Raab P, Hattingen E, Franz K, Zanella FE, Lanfermann H. Cerebral gliomas: diffusional kurtosis imaging analysis of microstructural differences. Radiology 2010;254:876–81.
12. Helpern JA, Adisetiyo V, Falangola MF, et al. Preliminary evidence of altered gray and white matter microstructural development in the frontal lobe of adolescents with attention-deficit hyperactivity disorder: a diffusional kurtosis imaging study. J Magn Reson Imaging 2011;33:17–23.
13. Falangola MF, Jensen JH, Babb JS, et al. Age-related non-Gaussian diffusion patterns in the prefrontal brain. J Magn Reson Imaging 2008;28:1345–50.
14. Knutson KL, Rathouz PJ, Yan LL, Liu K, Lauderdale DS. Stability of the Pittsburgh Sleep Quality Index and the Epworth Sleepiness Questionnaires over 1 year in early middle-aged adults: the CARDIA study. Sleep 2006;29:1503–6.
15. Beck AT, Epstein N, Brown G, Steer RA. An inventory for measuring clinical anxiety: psychometric properties. J Consult Clin Psychol 1988;56:893–7.
16. Beck AT, Steer RA, Ball R, Ranieri W. Comparison of Beck Depression Inventories -IA and -II in psychiatric outpatients. J Pers Assess 1996;67:588–97.
17. Nasreddine ZS, Phillips NA, Bedirian V, et al. The Montreal Cognitive Assessment, MoCA: a brief screening tool for mild cognitive impairment. J Am Geriatr Soc 2005;53:695–9.
18. Iber C, Ancoli-Israel S, Chesson A, Quan SF. The AASM manual for the scoring of sleep and associated events: rules, terminology and technical specifications. 1st ed. Westchester, IL: American Academy of Sleep Medicine, 2007.
19. Sleep-related breathing disorders in adults: recommendations for syndrome definition and measurement techniques in clinical research. The Report of an American Academy of Sleep Medicine Task Force. Sleep 1999;22:667–89.
20. Tabesh A, Jensen JH, Ardekani BA, Helpern JA. Estimation of tensors and tensor-derived measures in diffusional kurtosis imaging. Magn Reson Med 2011;65:823–36.
21. Rorden C, Karnath HO, Bonilha L. Improving lesion-symptom mapping. J Cogn Neurosci 2007;19:1081–8.
22. Ashburner J, Friston KJ. Unified segmentation. NeuroImage 2005;26:839–51.
23. Yadav SK, Kumar R, Macey PM, Woo MA, Yan-Go FL, Harper RM. Insular cortex metabolite changes in obstructive sleep apnea. Sleep 2014;37:951–8.
24. Kumar R, Birrer BV, Macey PM, et al. Reduced mammillary body volume in patients with obstructive sleep apnea. Neurosci Lett 2008;438:330–4.
25. Zhuo J, Xu S, Proctor JL, et al. Diffusion kurtosis as an in vivo imaging marker for reactive astrogliosis in traumatic brain injury. Neuroimage 2012;59:467–77.
26. Hui ES, Du F, Huang S, Shen Q, Duong TQ. Spatiotemporal dynamics of diffusional kurtosis, mean diffusivity and perfusion changes in experimental stroke. Brain Res 2012;1451:100–9.
27. Purkayastha S, Fadar O, Mehregan A, et al. Impaired cerebrovascular hemodynamics are associated with cerebral white matter damage. J Cereb Blood Flow Metab 2014;34:228–34.
28. Gupta A, Mayer EA, Sanmiguel CP, et al. Patterns of brain structural connectivity differentiate normal weight from overweight subjects. NeuroImage Clin 2015;7:506–17.
29. Salat DH, Williams VJ, Leritz EC, et al. Inter-individual variation in blood pressure is associated with regional white matter integrity in generally healthy older adults. Neuroimage 2012;59:181–92.
30. Bolzenius JD, Laidlaw DH, Cabeen RP, et al. Brain structure and cognitive correlates of body mass index in healthy older adults. Behav Brain Res 2015;278:342–7.
31. Jansen JF, Stambuk HE, Koutcher JA, Shukla-Dave A. Non-gaussian analysis of diffusion-weighted MR imaging in head and neck squamous cell carcinoma: a feasibility study. Am J Neuroradiol 2010;31:741–8.
32. Latt J, Nilsson M, Wirestam R, et al. Regional values of diffusional kurtosis estimates in the healthy brain. J Magn Reson Imaging 2013;37:610–8.
33. Verkhratsky A. Physiology and pathophysiology of the calcium store in the endoplasmic reticulum of neurons. Physiol Rev 2005;85:201–79.
34. Hachinski VC, Oppenheimer SM, Wilson JX, Guiraudon C, Cechetto DF. Asymmetry of sympathetic consequences of experimental stroke. Arch Neurol 1992;49:697–702.
35. Shoemaker JK, Norton KN, Baker J, Luchyshyn T. Forebrain organization for autonomic cardiovascular control. Auton Neurosci 2015;188:5–9.

ACKNOWLEDGMENTS

The authors thank Dr. Santosh K. Yadav, Mrs. Karen A. Harada, and Ms. Kelly A. Hickey for assistance with data collection, and Ms. Ruchi Vig for editorial help.

SUBMISSION & CORRESPONDENCE INFORMATION

Submitted for publication April, 2015
Submitted in final revised form July, 2015
Accepted for publication July, 2015

Address correspondence to: Rajesh Kumar, PhD, Department of Anesthesiology, David Geffen School of Medicine at UCLA, 56-141 CHS, 10833 Le Conte Avenue, University of California at Los Angeles, Los Angeles, CA 90095-1763; Tel: (310) 206-6133, (310) 206-1679; Fax: (310) 825-2236; Email: rkumar@mednet.ucla.edu

DISCLOSURE STATEMENT

This was not an industry supported study. This research work was supported by National Institutes of Health R01 HL113251 and R01NR015038. The authors have indicated no financial conflicts of interest.